Adaptive Thresholding for HF Radar Ship Detection

Anna L. Dzvonkovskaya and Hermann Rohling

Hamburg University of Technology, Institute of Telecommunications,
Eissendorfer Strasse 40, 21073 Hamburg, Germany

High frequency (HF) radars are capable to detect and track targets at extremely long ranges. But the signal environment that includes external noise, different kinds of clutter and interference will significantly limit the detection and system capability. This paper considers a new approach to solve the ship detection problem in a complex HF radar signal environment. It uses detection procedure based on conventional constant false-alarm-rate (CFAR) and curvilinear regression analysis of power spectrum values along range and Doppler cells for thresholding. The CFAR detection test rule was combined with a local peak determination procedure. The proposed detection scheme was tested using real HF radar data and gave very promising results.

1. INTRODUCTION

A high frequency (HF) radar, which is based on surface wave propagation provides a unique capability to detect targets far beyond the conventional microwave radar coverage. HF radars use the frequency band of 3…30 MHz to provide a large coverage that could extend more than 200 nautical miles in range. These maximum range values are of high interest and appear in consequence of the United Nations Convention on the Law of the Sea established 200 nautical miles as the Exclusive Economic Zone (EEZ). Continuous maritime surveillance of activity within a nation's EEZ is a key question in protection of national sovereignty.

It is well known that HF radar's performance depends on its ability to detect and track targets at long ranges and also to resolve closely spaced targets. But the signal environment of HF radar is significantly different from that of typical microwave radars. At HF band the environmental noise dominates the pure receiver noise, and the various sources of interference have different characteristics. The process of understanding these characteristics has lead to the development of effective mitigation techniques and optimal signal processing schemes for detection and tracking. However, the external noise and the interference levels will ultimately limit the detection range of the HF radar. Moreover, target detection procedures require relatively long coherent integration times to increase the signal-to-noise ratio. In this time period it is assumed that each target moves with a constant speed, which means the target does not accelerate or even maneuver significantly. Therefore the resulting spectral behavior of accelerating or maneuvering targets must be well understood if they are to be detected and tracked.

For ship detection and tracking procedures the sea clutter can be considered to be an unwanted, self-generated interference that is the result of the interaction of the radiated electromagnetic wave with ocean surface and ocean waves. The dominant contribution is produced by scatter from ocean waves having a wavelength, which is half of the radar wavelength and moving radially to and away from the radar site. This first-order resonant scattering effect results in two dominant peaks called Bragg lines (Barrick, 1972). Bragg resonant scattering will also occur at harmonics of the principal wavelength and results in second-order peaks in the spectrum. Another source of second-order scattering is caused by the interaction between crossing sea waves. If these crossing sea waves generate a third sea wave with a wavelength equal to one-half of the radar wavelength, then Bragg-resonance will occur. It is this condition that leads to an increase in the continuum level between the Bragg lines in the Doppler spectrum, and this is referred to as the second-order continuum. Therefore, the sea clutter can be characterized as a distributed, non-directional source.

Another type of clutter that appears in HF radar data occurs as a consequence of meteor reflections. The ionized gas trail produced by meteoroids entering the Earth's atmosphere produces large radar echoes that can degrade the radar detection performance. Meteor echoes are characterized by a wide Doppler spread of relatively short duration. Meteoroid based radar echo signal are characterized by a pulse-like echo that rises rapidly to a maximum amplitude and decays over a few

seconds. Meteor echoes can potentially degrade the HF radar detection performance by masking target echoes having similar Doppler frequency shifts. In addition they can result in false alarms, because their spectral characteristics are very similar to those of a maneuvering target. Fortunately echo signals from meteor trails do not form target tracks in general.

For a ship that travels at a constant velocity within a coherent integration time interval, the echo signal is characterized by an impulse like Doppler frequency spectrum and fulfils the point target assumption. For any target, which radial velocity changes within the coherent integration period, the echo signal is characterized by spectral components that are smeared over several Doppler frequency bins. For this situation special handling routines are required in both the target detection and tracking processes.

2. PROPOSED ADAPTIVE TEST STATISTICS FOR DETECTION ALGORITHM

Ship detection using a constant false-alarm-rate (CFAR) algorithm follows the beamforming process in a HF radar data processing chain. The typical HF echo signal environment is shown in Figure 1 and illustrates the complexity of the target detection process. Here the Doppler frequency spectra of the radar returns from all range gates are shown. Most of the observed signal components are labelled in Figure 1, which includes sea clutter (resonant scattering of the first and second order), meteor clutter, noise, land reflections and some ship targets. Due to the complexity of the real signal environment it is desirable to employ adaptive procedures in the detection process to accommodate clutter, noise and interference levels that vary from coherent integration time to coherent integration time as well as from cell to cell.

The probability of detection is a measure of the likelihood that a target with a given SNR will be detected. The probability of false alarm is determined by the likelihood that the noise or clutter signal amplitude exceeds a given level.

We consider a set of Range-Doppler-Azimuth processed radar data corresponding to a single snapshot collected by the HF radar. Further we apply the detection algorithm to Range-Doppler (RD) power spectrum map for a given azimuth beam index. The RD map statistics may vary from snapshot to snapshot therefore we have to detect targets against a background signal which has an unknown distribution.

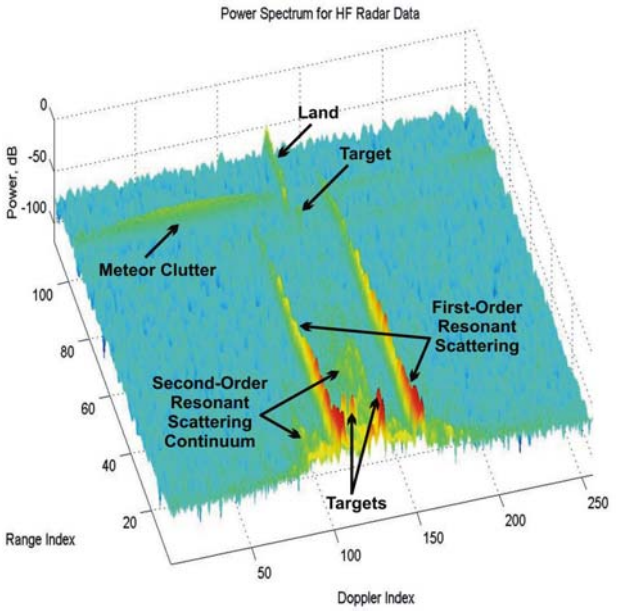

Figure 1. HF radar power spectrum example including some targets and different kinds of clutter.

Detection of a target signal can be expressed with hypotheses H_0 (no target is present) and H_1 (target is present). CFAR methods usually formulate a test statistic for each cell of interest and compare it to some threshold (Rohling, 1983). The CFAR threshold calculation is usually based on the Neyman-Pearson criterion with a fixed probability P_{fa} of false alarm and a maximum probability of target detection. A detection decision must be made for each RD cell individually.

We applied the conventional curvilinear regression analysis (Kendall and Stuart, 1967) to a logarithmic scaled power spectrum along the range and Doppler cells respectively. The examples of regression curves and their upper confidential bounds are shown in Figures 2 and 3.

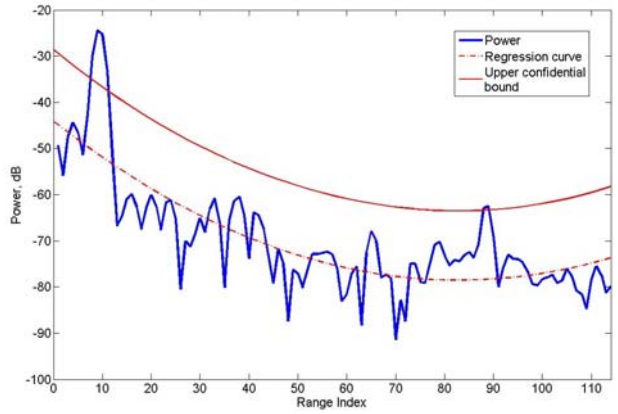

Figure 2. Example of power spectrum with regression curve along range cells.

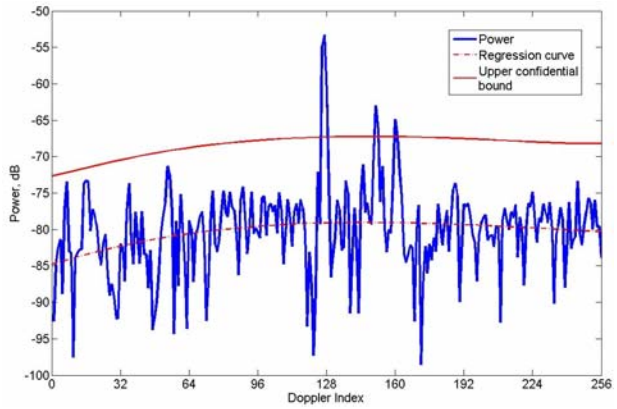

Figure 3. Examples of power spectrum with regression curves along Doppler frequency cells.

Let $T_{\alpha,ran}$ be 100(1 - α)% upper confidential bound value for the power regression curve along range and $T_{\alpha,Dop}$ be 100(1 - α)% upper confidential bound value for the power regression curve along Doppler frequency. The adaptive threshold *T* at the specified test cell is set as

$$T = \max\{T_{\alpha,ran},\ T_{\alpha,Dop}\}. \qquad (1)$$

The RD test cell value *Y* is compared with the threshold *T* using the test rule

$$Y \underset{\text{No target}}{\overset{\text{Target}}{\gtrless}} T. \qquad (2)$$

Due to applying windowing functions in radar data processing the test decision can be spread over several adjacent cells. To eliminate this effect we use an additional technique proposed in (Turley, 1997) to determine local peaks on RD map. We construct additional rule

$$Y \underset{\text{No target}}{\overset{\text{Target}}{\gtrless}} \max_{\substack{1\le i\le n,\\ 1\le j\le m}} \{X_{i,j}\} \qquad (3)$$

where the set of power values $\{X_{i,j}\}$ is formed from the RD cells that surround the test cell *Y* within a given frame of $n \times m$ cells.

The final hybrid decision about target presence is made if test rules (2) and (3) result in the same detection decision simultaneously.

3. TEST RESULTS

We tested the proposed detection algorithm on the real raw data from HF radar system WERA developed at the University of Hamburg, Germany (Gurgel *et al*., 2001). The coherent integration time of a single snapshot was about 67 seconds for each range gate. For the data processing technique we used Hamming windowing function both for FFT and beamforming process. Examples of RD power spectrum map for the specified azimuth values are shown in Figures 4 and 5. It can be seen in these figures that several kinds of clutter mentioned above are presented. Figure 4 also includes the meteor clutter among the others. Obviously the detection task is still complicated to solve in this specific environment.

We used regression with polynom of the 2nd order along range cells and regression with polynom of the 3rd order along Doppler cells with α = 0.05 for both upper confidential bounds and calculated the threshold (1) for each RD cell. Further we tested with the test rules (2) and (3). The final decisions of target positions are shown on the RD map with black dots (see Figures 6 and 7). For comparison we also applied the well-known Greatest of Selection in Cell Averaging (GOCA) CFAR technique mentioned in (Turley, 1997). The results for the same RD map are shown in Figures 8 and 9.

4. CONCLUSION

This paper presented a new approach based on the adaptive power regression thresholding separately for Doppler frequency and range cells. The approach is combined with the local peak determination procedure to solve the target detection problem in complex HF radar signal environment. The obtained results show the acceptability of the proposed algorithm.

Acknowledgements. The authors would like to thank Dr. Gurgel for the presented real data of HF radar system WERA developed at the University of Hamburg, Germany, that made it possible to provide the analysis of proposed detection algorithm.

REFERENCES

Barrick D., First-Order Theory and Analysis of MF/HF/VHF Scatter from the Sea, IEEE Transactions on Antennas and Propagation, 1972, Vol. AP-20, No.1, pp. 2-10.

Rohling H., Radar CFAR Thresholding in Clutter and Multiple Target Situations, IEEE Transactions on Aerospace and Electronic Systems, 1983, Vol. AES-19, No.4, pp. 608-621.

Kendall M.G., A. Stuart, The Advanced Theory of Statistics, Vol. 2, Charles Griffin and Company Ltd., London, 1967.

Turley M.D.E., Hybrid CFAR Techniques for HF Radar, Radar-97 (Conf. Publ. No. 449), pp.36-40, Edinburgh, UK, 1997.

Gurgel K.-W., H.-H. Essen, and T. Schlick, The

University of Hamburg WERA HF Radar – Theory and Solutions, First International Radiowave Oceanography Workshop Proceedings (ROW-2001), pp. 19-25, Oregon, USA, 2001.

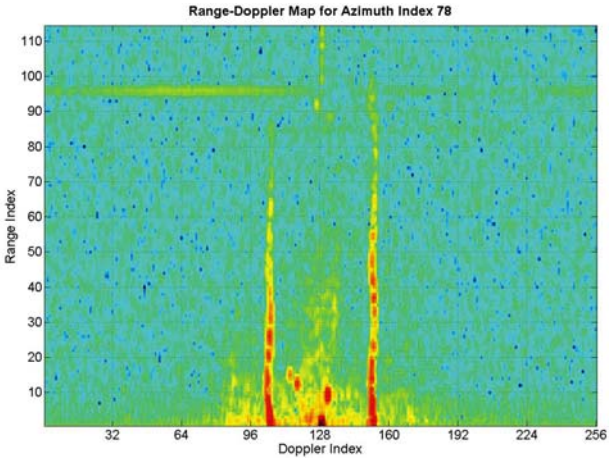

Figure 4. RD map for azimuth index 78.

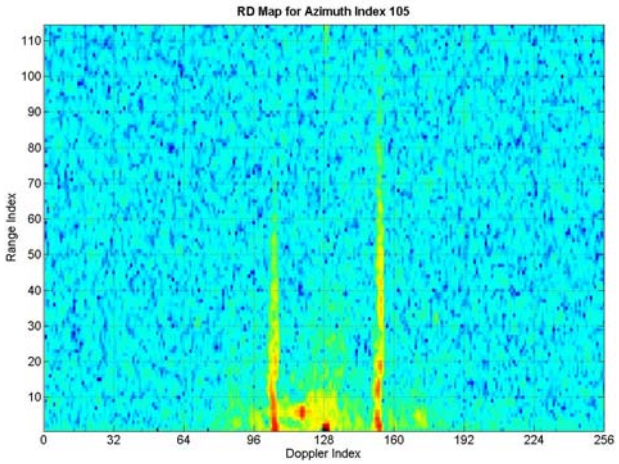

Figure 5. RD map for azimuth index 105.

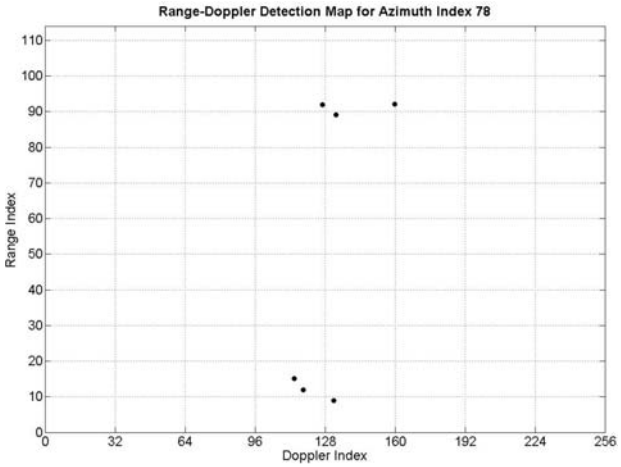

Figure 6. RD detection map for azimuth index 78 (proposed technique).

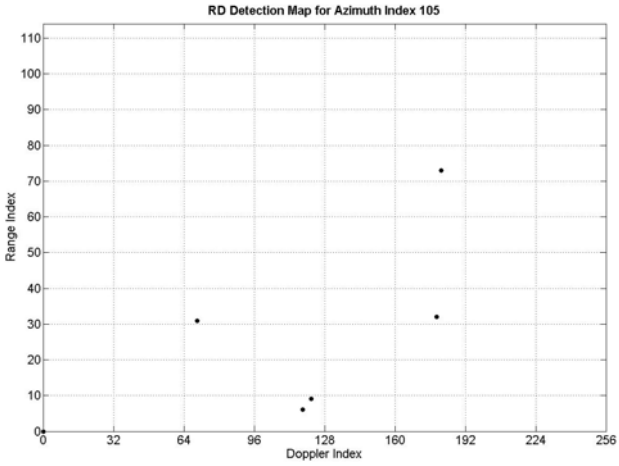

Figure 8. RD detection map for azimuth index 105 (proposed technique).

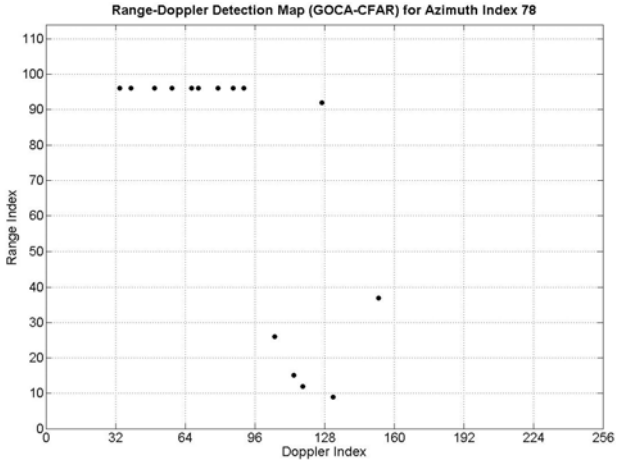

Figure 7. RD detection map for azimuth index 78 (GOCA-CFAR technique).

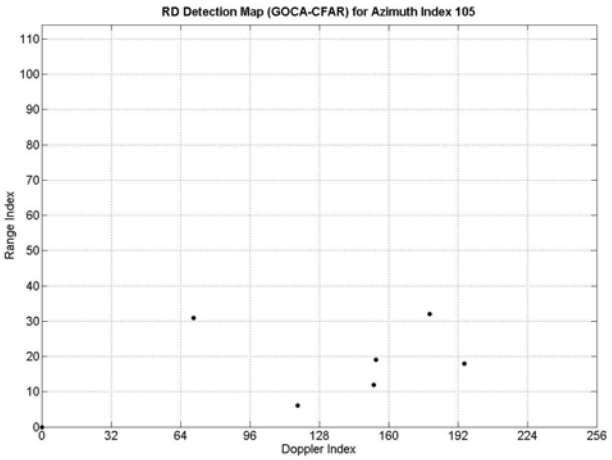

Figure 9. RD detection map for azimuth index 105 (GOCA-CFAR technique).